

IT-Yb1 Optical Lattice Clock: Absolute Frequency Measurement at the Cs Fountain Uncertainty Level

Original

IT-Yb1 Optical Lattice Clock: Absolute Frequency Measurement at the Cs Fountain Uncertainty Level / Goti, I.; Condio, S.; Clivati, C.; Risaro, M.; Gozzelino, M.; Costanzo, G. A.; Levi, F.; Calonico, D.; Pizzocaro, M.. - ELETTRONICO. - (2023). (2023 Joint Conference of the European Frequency and Time Forum and IEEE International Frequency Control Symposium (EFTF/IFCS) Toyama, Japan 15-19 May 2023) [10.1109/efft/ifcs57587.2023.10272188].

Availability:

This version is available at: 11583/2987228 since: 2024-03-27T16:57:32Z

Publisher:

IEEE

Published

DOI:10.1109/efft/ifcs57587.2023.10272188

Terms of use:

This article is made available under terms and conditions as specified in the corresponding bibliographic description in the repository

Publisher copyright




IEEE postprint/Author's Accepted Manuscript

©2023 IEEE. Personal use of this material is permitted. Permission from IEEE must be obtained for all other uses, in any current or future media, including reprinting/republishing this material for advertising or promotional purposes, creating new collecting works, for resale or lists, or reuse of any copyrighted component of this work in other works.

(Article begins on next page)

Article

3D Multispectral Imaging for Cultural Heritage Preservation: The Case Study of a Wooden Sculpture of the Museo Egizio di Torino

Leila Es Sebar ^{1,*}, Luca Lombardo ², Paola Buscaglia ^{1,3}, Tiziana Cavaleri ^{3,4}, Alessandro Lo Giudice ^{5,6}, Alessandro Re ^{5,6}, Matilde Borla ⁷, Sara Aicardi ⁸ and Sabrina Grassini ¹

¹ Department of Applied Science and Technology, Politecnico di Torino, 10129 Turin, Italy

² Department of Electronics and Telecommunications, Politecnico di Torino, 10129 Turin, Italy

³ Centro Conservazione e Restauro “La Venaria Reale”, 10078 Venaria Reale, Italy

⁴ Dipartimento di Economia, Ingegneria, Società e Impresa, Università degli Studi della Tuscia, 01100 Viterbo, Italy

⁵ Dipartimento di Fisica, Università degli Studi di Torino, 10125 Turin, Italy

⁶ Istituto Nazionale di Fisica Nucleare (INFN), Sezione di Torino, 10125 Turin, Italy

⁷ Soprintendenza Archeologia, Belle Arti e Paesaggio per la città Metropolitana di Torino, 10122 Turin, Italy

⁸ Museo Egizio di Torino, 10123 Turin, Italy

* Correspondence: leila.essebar@polito.it

Abstract: Digitalization techniques, such as photogrammetry (PG), are attracting the interest of experts in the cultural heritage field, as they enable the creation of three-dimensional virtual replicas of historical artifacts with 2D digital images. Indeed, PG allows for acquiring data regarding the overall appearance of an artifact, its geometry, and its texture. Furthermore, among several image-based techniques exploited for the conservation of works of art, multispectral imaging (MSI) finds great application in the study of the materials of historical items, taking advantage of the different responses of materials when exposed to specific wavelengths. Despite their great usefulness, PG and MSI are often used as separate tools. Integrating radiometric and geometrical data can notably expand the information carried by a 3D model. Therefore, this paper presents a novel research methodology that enables the acquisition of multispectral 3D models, combining the outcomes of PG and MSI (Visible (VIS), Ultraviolet-induced Visible Luminescence (UVL), Ultraviolet-Reflected (UVR), and Ultraviolet-Reflected False Color (UVR-FC) imaging) in a single coordinate system, using an affordable tunable set-up and open-source software. The approach has been employed for the study of two wooden artifacts from the Museo Egizio di Torino to investigate the materials present on the surface and provide information that could support the design of suitable conservation treatments.

Keywords: photogrammetry; multispectral imaging; data fusion; 3D multispectral model; digitalization; cultural heritage; digital twin; digital methods



Citation: Es Sebar, L.; Lombardo, L.; Buscaglia, P.; Cavaleri, T.; Lo Giudice, A.; Re, A.; Borla, M.; Aicardi, S.; Grassini, S. 3D Multispectral Imaging for Cultural Heritage Preservation: The Case Study of a Wooden Sculpture of the Museo Egizio di Torino. *Heritage* **2023**, *6*, 2783–2795. <https://doi.org/10.3390/heritage6030148>

Academic Editor: Fabrizio Antonelli

Received: 31 January 2023

Revised: 24 February 2023

Accepted: 2 March 2023

Published: 7 March 2023



Copyright: © 2023 by the authors. Licensee MDPI, Basel, Switzerland. This article is an open access article distributed under the terms and conditions of the Creative Commons Attribution (CC BY) license (<https://creativecommons.org/licenses/by/4.0/>).

1. Introduction

The study of artifacts belonging to the field of Cultural Heritage (CH) has always been a challenging task. Indeed the methodologies aimed at studying such artifacts require several conditions to be satisfied to avoid any possible damage to the items. When possible, it has to be preferred to investigate an artifact using techniques that can be non-invasive, i.e., involving no sampling, and that can be performed where the object is stored or exhibited [1]. Therefore, there is increasing interest in the development and application of analytical techniques that can satisfy the above-mentioned requirements and provide useful insights into the state of artwork preservation [2].

In this context, digitalization techniques are gathering the interest of experts in the field of Cultural Heritage. The creation of a 3D model of artifacts, without doubt, brings several advantages. Firstly, the possibility of fully documenting an item and creating a

trustworthy digital replica, which includes data regarding the overall aspect, color, texture, morphology, and geometry of an artifact. Secondly, digital twins of artifacts can then be exploited in several ways. First, the replica can be archived to virtually preserve an artifact and monitor its state of preservation over time, in consideration of future degradation or non-predictable damage or loss. 3D models can also be employed as an active tool for the study of an artifact: they can be used to document and monitor the morphology and aspect of an item, along with its conservation or during interventions, as traditionally done with 2D technical imaging, but with the advantage of having a model that can be virtually manipulated. In addition, 3D models can be shared among institutions, such as research or conservation centers, to transfer information about an artifact during its investigation. Moreover, a virtual replica also finds applications among the public, enabling virtual access to items from all over the world. Eventually, 3D models can even be employed to create 3D-printed replicas of an artifact that can be exploited to create more inclusive tactile exhibitions or for innovative displays [3–9].

Considering all the potentiality that a 3D model carries, several digitalization techniques have been employed over the last years in the Cultural Heritage field, with a particular focus on the non-contact methodologies that enable modeling from reality through light waves [3].

Among a large variety of techniques, such as laser scanning, structured light, 3D scanners, and many more, photogrammetry finds major applications [10–12]. Indeed, this technique enables the creation of high-resolution 3D models with accurate geometrical information compared to other digitalization processes [12,13]. In addition, it allows the creation of textured models that reproduce the photorealistic aspect of an item. Furthermore, photogrammetry can be performed on objects of small to large size and can be easily carried out in situ without relevant changes to the employed instrumentation [14].

The vast group of techniques employed for the diagnostic and characterization of materials and surfaces, such as computed tomography, electronic microscopy, X-ray fluorescence, and Raman Spectroscopy [2,15–21], also includes Multispectral Imaging techniques (MSI), often employed to investigate the outermost layers of items, including the ones in the Cultural Heritage field. Indeed, MSI has proven to be successful in the preliminary mapping the distribution of pigments, varnishes, underdrawings, and the overall constituent materials of an item. This is possible since images are acquired by selecting specific ranges of the electromagnetic spectrum and by illuminating with sources of certain wavelengths. The radiation employed to investigate a surface can be absorbed, reflected, and/or emitted as luminescence radiation. In addition, radiation from different spectral regions has a different penetration power. These features enable the study of painted surfaces and highlight details that are not detectable by the human eye [8,18,22–28]. Today, thanks to the development of new and advanced technologies, multispectral imaging has improved regarding resolution, sensitivity, portability, and cost. Indeed, the instrumentation is becoming more affordable and accessible to a larger user base [14]. For example, once modified, commercial digital cameras can acquire signals on a wider range of the electromagnetic spectrum.

It is worth underlining that providing the conservators with scientific and diagnostic information is of outstanding importance for conservation treatments. At the same time, providing conservators and experts with analytical data and results that are easy to read can improve the decision-making process. In this context, 3D models could support the display of scientific results. Indeed, the applicability and potentiality of 3D models as diagnostic tools in the Cultural Heritage field could be enhanced by the possibility of integrating data coming from different techniques on a 3D model [26,29]. In particular, the idea of combining the results of techniques that are usually employed as separate tools, such as photogrammetry and multispectral imaging, could notably expand the information carried by a 3D model.

Recent studies present different approaches to combine multispectral information and 3D models [14,30,31]. For instance, in [30], a 3D model of a sculpture showing the

distribution of Egyptian blue by visible-induced infrared luminescence (VIL) imaging has been created. Furthermore, the study presented by [14] deals with a methodology aiming to combine photogrammetry and spectral imagery to study two artifacts. The methodology proposed by the authors involves using a modified digital single-lens reflex (DSLR) camera coupled with a sophisticated and expensive lens that makes refocusing unnecessary when switching wavelengths. In addition, the 3D model is constructed utilizing commercial software, i.e., Agisoft Metashape (Agisoft Photoscan Pro 1.4.2). Also, in [31], a similar approach was presented to study a polychrome Hellenistic terracotta funerary head vase, creating three item models. In this case, separated 3D models were built using Agisoft PhotoScan Professional (Agisoft Metashape) after masking the RGB images and applying the same masks to the image sets used for the luminescence-textured 3D models. Indeed, several studies are based on commercial software, such as Agisoft PhotoScan Professional [14,31–33].

This study aims to present a user-friendly approach, with accessible equipment and software, that can be tuned to be applied and replicated both in laboratories or where the artifacts are stored or displayed, such as in museums. In addition, the present study is focused on an innovative approach to integrating geometrical and spatial information coming from PG and radiometric data collected with MSI in a unique 3D model that allows navigating the collected data in a single coordinate system. The aim is to avoid the creation of separated 3D models that need to be successively aligned and allows the re-texturing of a geometrically accurate 3D model extracted from VIS images.

This approach employs affordable and portable instrumentation that can be tuned to meet users' needs and involves a simple pipeline and the use of open-source software that allows one to carry out all the required image processing. The final aim is the creation of multispectral 3D models that can be exploited as an active tool for the artifact study to be integrated into the practices for the conservation of artifacts in the CH field.

The proposed approach was employed to investigate two artifact parts of a wooden sculpture that belongs to the collection of the Museo Egizio di Torino. In particular, the combination of multispectral imaging (visible (VIS), Ultraviolet-induced Visible Luminescence (UVL), Ultraviolet-reflected (UVR) and Ultraviolet-reflected False Color (UVR-FC) imaging) and photogrammetry was exploited to investigate the materials of the surface, characterize any discontinuities, and detect any organic materials applied in previous interventions to provide the conservators with information that could be of support in the development of conservation treatments.

Furthermore, additional analyses were carried out on the artifacts to support and confirm the results obtained with the proposed approach. In particular, portable non-invasive X-ray fluorescence spectroscopy (XRF) and micro-invasive Fourier-transform infrared (FTIR) spectroscopy were carried out to study both the original pigments and materials of past conservation treatments.

The present study is part of a wide project related to characterizing the state of preservation of several Egyptian wooden sculptures of the Museo Egizio di Torino. The project involved the characterization of the constituent materials of the artifacts, together with possible deposits on the surface and modern materials that could have been applied in previous interventions. All this information is gathered to enable the definition of the most appropriate methodological approach for conservation treatments.

2. Materials and Methods

2.1. The Artifacts

This paper focuses on the study of a wooden model of a granary (S. 08651) from the collection of the Museo Egizio di Torino (from Asyut–Egypt–Schiaparelli excavation 1908). In Figure 1a,b, a visible (VIS) image of respectively a side and top view of the artifact is shown. The entire artifact dates back to the Middle Kingdom (1939–1875 BC) and depicts a scene of everyday life set indoors. This kind of artwork can usually be found as part of the funerary ensembles belonging to the Middle Kingdom, and its function is

to represent a scene of daily life [34]. Indeed, it is composed of several parts, namely the main quadrangular element, multiple smaller elements, such as a door, staircases, a floor, and some sacks of wheat and figures placed within the scene. The sculptures used to be placed in the funerary ensemble to help the tomb owner collect food necessary for survival in the afterlife. On the other hand, they could also represent the people working for the tomb owner.



Figure 1. VIS image of the artifact from the collection of the Museo Egizio di Torino—Middle Kingdom, beginning of the XXII dynasty (1939–1875 BC): (a) side view; (b): top view.

The sculptures are painted with a palette composed of a few pigments, namely red, black, and yellow.

Concerning the state of preservation of the whole artifact, it is possible to observe the presence on the surface of several deposits and particulates, together with several cracks in the material and stratigraphy of the decorations. Furthermore, the surface presents abrasions and some detachment. Therefore, the whole artifact had to undergo interventions, in particular, cleaning treatments to remove all the deposited materials on the surface.

Among all the figures and elements that are part of the whole artifact, this paper will mainly focus on two particular sculptures, namely the two sacks of wheat depicted in Figures 2 and 3. For clarity, the two sculptures will be referred to in the following as sack No. 1 and sack No. 2.



Figure 2. VIS images of the wooden sculpture of the sack No. 1: (a) front view, and (b) back view. The white arrow indicates where the micro-sample was collected for Fourier-transform infrared (FTIR) spectroscopy analysis.



Figure 3. VIS images of the wooden sculpture of the sack No. 2: (a) front view, and (b) back view. The white arrow indicates where the micro-sample was collected for Fourier-transform infrared (FTIR) spectroscopy analysis.

These two items are of particular interest for the methodology presented in this manuscript since their surface is characterized by the presence of layered superficial substances. In addition, one of the aims was to detect the presence of any aged material on the surface, considering both original products and ones that could have been applied in previous interventions to protect the surface. These materials are usually organic and, therefore, are characterized by a luminescence response to ultraviolet (UV) sources. As a matter of fact, in multispectral imaging, UV radiation finds great use in the study of most external layers due to its low penetration power, and in particular, for the study of varnishes and coatings.

The combined use of ultraviolet imaging techniques such as UVL and UVR imaging, and photogrammetry can enable the characterization and mapping of the finishing on the surfaces. Furthermore, a UVR-FC 3D model can enhance the clarity and legibility of such information. To this aim, the following section presents the setup employed for generating the multispectral 3D models of the sculptures of the two sacks of wheat.

2.2. Analytical Approach for Multispectral 3D Model by Photogrammetry

To investigate the artifacts and integrate both radiometric and geometrical data in a unique 3D model, a specific set-up was employed. In particular, photogrammetry can be performed in two configurations, namely, keeping the object still and acquiring images by moving the camera around it or keeping the camera in a fixed position and placing the object on a turntable. To the aim of this study, the latter configuration was employed, placing the camera on a tripod. This assures that the camera and item relative orientation do not change during the acquisition. Therefore, it is possible to acquire images that can be compared and overlapped, when exploiting different multispectral imaging techniques.

Therefore, the employed set-up is composed of several elements: (i) a modified digital camera, (ii) a rotating platform, (iii) radiation sources, (iv) filters.

For this study, an off-the-shelf digital camera modified to be sensitive to radiation in the range between 350 nm and 1100 nm has been employed. To this aim, the IR-blocking hot mirror was removed from a mirrorless camera, i.e., the Fujifilm XT-30 (APS-C X-Trans 1 CMOS 4 sensor). The camera was coupled with a prime lens with a fixed focal length (Minolta MC Rokkor-PF 50mm f/1.7). Tables 1 and 2 report the specifications of the camera and lens employed, respectively.

To ensure the best condition for the reconstruction of the 3D model, i.e., to enable the identification of the greatest number of homologous points between images, the camera parameters during the acquisition have to remain fixed. In particular, the illumination condition has to remain stable during the acquisition, together with the shutter speed, ISO values, aperture, and focal length. The employed parameters are reported in Table 3.

Table 1. Fujifilm XT-30 camera specifications.

Fujifilm XT-30	
Image size (pixels)	4608 × 3072
Effective megapixels	26.1
Sensor size, type	23.5 mm × 15.6 mm (APS-C) X-Trans CMOS 4
Pixel size (µm)	4.94
ISO range	160–12,800

Table 2. Minolta MC Rokkor-PF 50 mm f/1.7 prime lens specifications.

Minolta MC Rokkor-PF 50 mm f/1.7	
Focal length	50 mm
Minimum aperture	f/1.7
Maximum aperture	f/16
Focus type	Manual
Type	Prime

Table 3. Parameters employed for the acquisition of the visible (VIS), Ultraviolet-induced Visible Luminescence (UVL), and Ultraviolet-reflected (UVR) images of the artifacts.

Parameter	Value		
	VIS	UVL	UVR
Shutter Speed	1 s	20 s	20 s
Step angle		10	
ISO		200	
Image size		6240 × 4160	
Image Format		RAW	
Focal Length		50 mm	
Aperture		f/16	

The artifacts were placed on a precision rotation platform, the URS 150 BCC (Newport Corporation, Irvine, CA, USA). This platform has a payload capacity of 300 N, an angular resolution of 0.002°, bi-directional repeatability of $\pm 0.0044^\circ$, and can continuously rotate from 0° to 360°, enabling accurate positioning of the artifacts.

Several lighting sources and filters were employed, as required by the specific MSI technique. For VIS images, two tungsten-halogen lamps (800 W) were placed symmetrically at 45° concerning the object's surface. Furthermore, the HOYA UV&IR Cut visible bandpass filter was employed to select the signal in the visible region (400–700 nm), together with a 455 nm long-pass filter. For UVL and UVR images, two 365 nm UV LED sources (3000 mW AC/battery operated) were used. For UVL images, the HOYA UV&IR Cut visible bandpass filter was employed, while for UVR images, a Baader U-filter, with a transmission bandwidth of 60 nm (320–380 nm), was exploited to exclude the signal in the visible and IR regions (400–1100 nm). A 24-color X-Rite ColorChecker Classic Mini® was included in the scene to perform chromatic and exposure correction.

For the reconstruction of the 3D model, Meshroom [35], an open-source 3D reconstruction software based on the AliceVision® framework, was employed. This software has the advantage of being open-source and of consenting to carry on all the photogrammetry pipeline, from the image alignment to the textured 3D model. The pipeline can be used with the default setting by the user, but it can also be modified and configured to meet the user and project needs. Indeed, the pipeline comprises several processing blocks for every reconstruction step.

To create a unique 3D model that carries morphological and geometrical data from photogrammetry and radiometric data from MSI techniques, the pipeline was set as follows. The mesh and point cloud were generated using the embedded default pipeline, starting from the VIS images. Then the point cloud and mesh generated with the above-mentioned

step were employed to re-texture the VIS 3D model with the images from UVL, UVR, and UVR-FC techniques. In particular, the dense scene node is duplicated, and it is recomputed with a different set of images, i.e., UVL, UVR, UVR-FC, etc. It is worth underlying that this was possible since all the images were acquired by keeping the relative orientation of the camera and object stable during the acquisition. Consequently, this approach leads to the generation of a multispectral 3D model, which stores different data, with the advantage of keeping all the information in a single coordinate system, allowing one to navigate and compare the results as superimposed layers.

2.3. X-ray Fluorescence Spectroscopy and Micro-Invasive Fourier-Transform Infrared Spectroscopy

In addition to the imaging campaign, portable non-invasive X-ray fluorescence spectroscopy and micro-invasive Fourier-transform infrared spectroscopy were carried out to study both the original pigments and materials of past conservation treatments. Indeed, these analyses can support and confirm the results obtained with the proposed imaging approach.

XRF analysis was performed using a Micro-EDXRF Bruker Artax 200 spectrometer equipped with a fine focus X-ray source, including a molybdenum anode and a Si(Li) silicon drift detector (SDD) with an 8 μm beryllium window, providing an average resolution of approximately 144 eV for the full width at half maximum of the manganese *K α* line. The system includes a 4096-channel analog-to-digital converter (ADC), a series of interchangeable filters, and two 0.65 mm and 1.5 mm collimators to adjust spot analysis size. Maximum voltage and current are 50 kV and 1500 μA , respectively, for a maximum power of 40 W. In the present case, measurements were carried out using 30 kV voltage, 1300 μA current, 60 s acquisition time, and 1.5 mm collimator, with no filter, by fluxing helium gas onto the measurement area to improve the technique's detection limits (corresponding, with a helium flux, to $Z = 11$, sodium).

FTIR analysis was performed with a Bruker Vertex 70 FTIR spectrometer coupled with a Bruker Hyperion 3000 infrared microscope and equipped with a mercury cadmium telluride (MCT) detector. In particular, two micro-samples were collected from the surface of both artifacts, in correspondence with the points highlighted with a white arrow in Figures 2 and 3. Upon compression in a diamond cell, samples were analyzed as bulk in transmission mode through a 15 objective. Data were collected in the 650–4000 cm^{-1} spectral range, at a spectral resolution of 4 cm^{-1} , as the sum of 32 scans. Spectra were interpreted by comparison with published literature and spectral libraries available at the scientific laboratories of the Centro Conservazione e Restauro “La Venaria Reale”.

3. Results and Discussion

Portable non-invasive X-ray fluorescence spectroscopy (XRF) and micro-invasive Fourier-transform infrared (FTIR) spectroscopy were exploited to study both the original pigments and investigate the materials that could have been applied in previous conservation treatments.

The XRF analysis on representative areas of the different colors (white, yellow, and red, not compromised by restoration interventions) allowed for confirming the use of calcium carbonate, gypsum, red earth, and yellow earth, as traditional in the ancient Egypt palette [36].

The FTIR analysis carried out on the two samples removed from the wooden sack provided comparable results. A representative spectrum is reported in Figure 4. The FTIR analysis indicates the presence of calcite (2513, 1795, 1417, 877, and 713 cm^{-1}), gypsum (3394, 1620, 1164 cm^{-1}), and kaolin (3695, 3617, 1063, 1027, 913, 798, and 780 cm^{-1}). The analysis did not allow us to ascertain, nor to exclude, the presence of any natural finishes; however, the FTIR signals of oxalates were detected (1653 and 1323 cm^{-1}) as actually attributable to the degradation of organic substances. The signals at 1653 cm^{-1} and 1281 cm^{-1} suggest the possible presence of cellulose nitrate, while the signal at 1731 cm^{-1} may be associated with the presence of another organic substance, probably of synthetic origin.

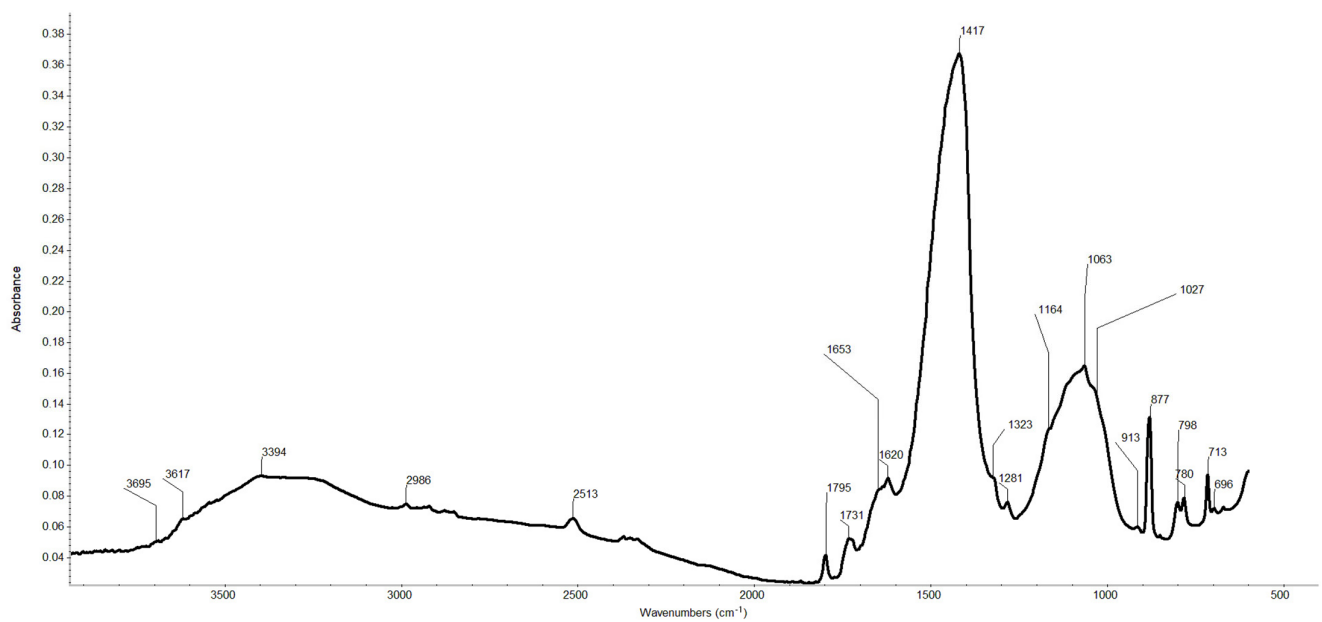


Figure 4. Representative FTIR spectrum acquired on the micro-samples collected from the two artifacts, in correspondence with the points highlighted with a white arrow in Figures 2 and 3.

The imaging approach presented in this study enabled the construction of multi-spectral 3D models, which integrated geometrical and morphological data acquired by photogrammetry and radiometric data collected with multispectral imaging. Some views of the multispectral 3D models of the artifacts are reported in Figures 5 and 6.

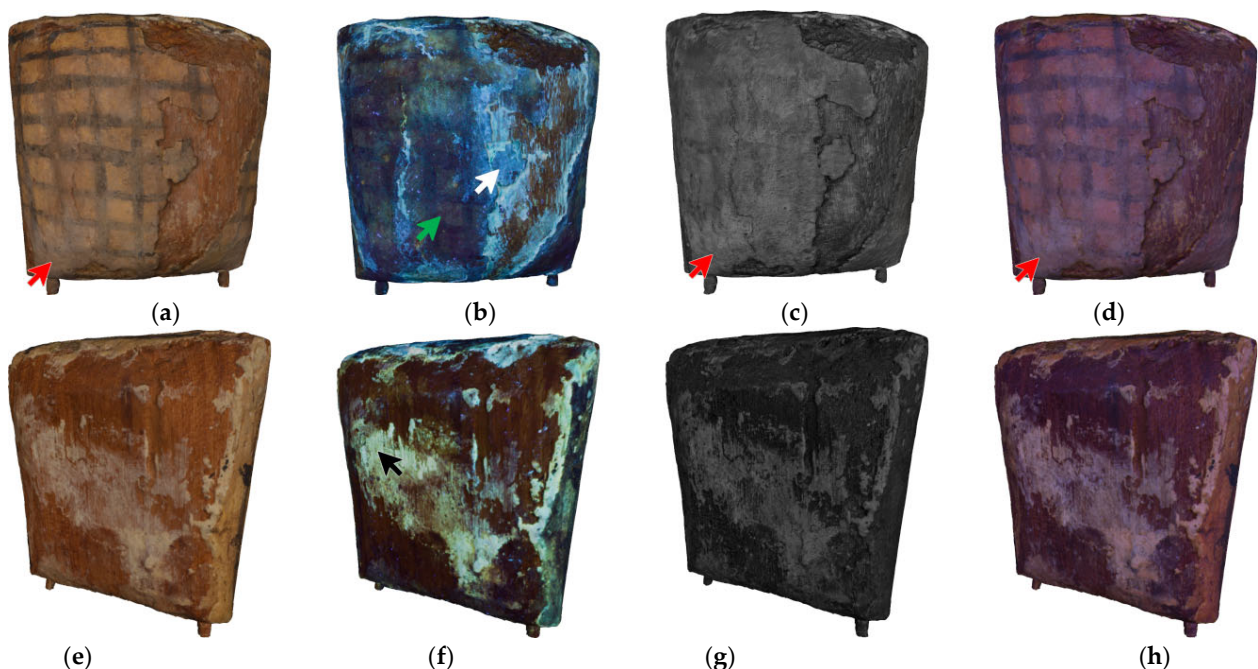


Figure 5. 3D models of wooden sack sculpture No. 1 by multispectral photogrammetry: (a) front view, VIS 3D model, (b) front view, UVL 3D model, (c) front view, UVR 3D model, (d) front view, UVR-FC 3D model, (e) back view, VIS 3D model, (f) back view, UVL 3D model, (g) back view, UVR 3D model, (h) back view, UVR-FC 3D model. White arrow: a bright light-blueish fluorescence, synthetic materials as a consolidant. Green arrow: blueish response, possible presence of cellulose nitrate and other organic substance, probably of synthetic origin. Black arrow: yellow fluorescence, preparation layer. Red arrows: whitish deposits detected in VIS, UVR and UVR-FC models.

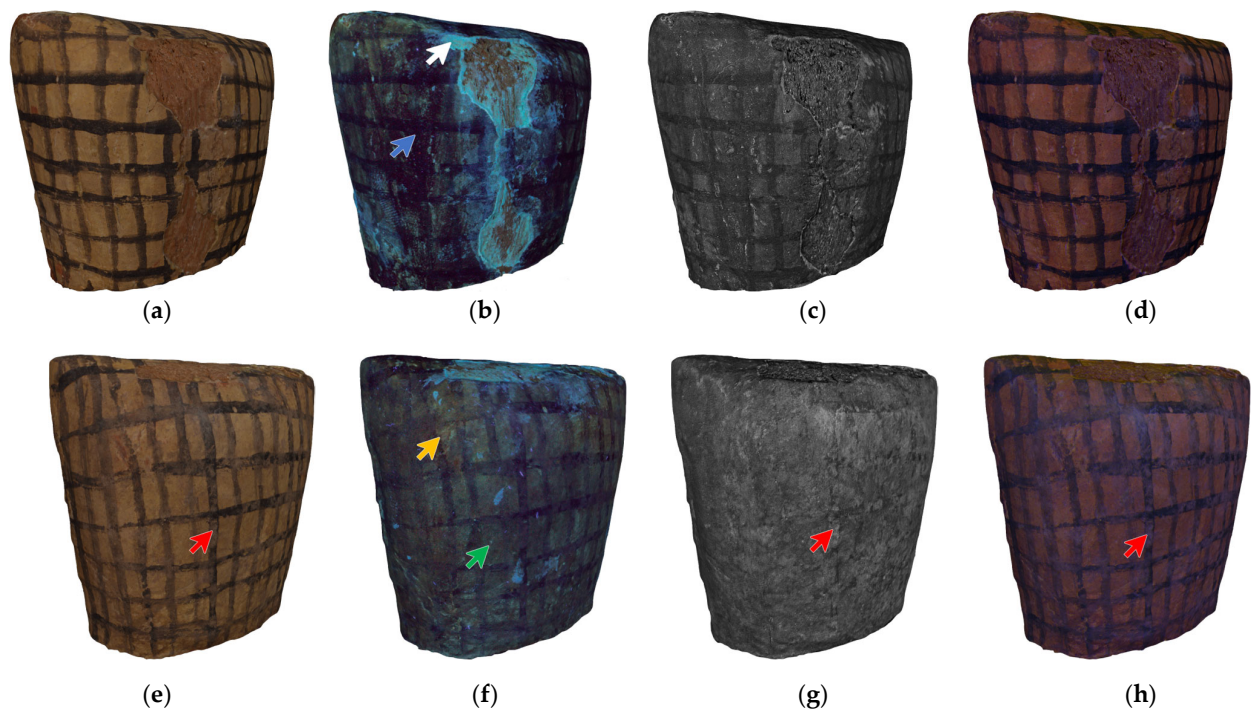


Figure 6. 3D models of wooden sack sculpture No. 2 by multispectral photogrammetry: (a) front view, VIS 3D model, (b) front view, UVL 3D model, (c) front view, UVR 3D model, (d) front view, UVR-FC 3D model, (e) back view, VIS 3D model, (f) back view, UVL 3D model, (g) back view, UVR 3D model, (h) back view, UVR-FC 3D model. White arrow: a bright light-blueish fluorescence, synthetic materials as a consolidant. Blue arrow: dark response, non-fluorescent material. Green arrow: blueish response, possible presence of cellulose nitrate and other organic substance, probably of synthetic origin. Yellow arrow: yellowish response, absence of coating or varnishes. Red arrows: whitish deposits detected in VIS, UVR and UVR-FC models.

The combination of the above-mentioned data allows conservators to deepen their knowledge of the state of preservation of the artifacts, to observe in detail the distribution of materials on the surface, and to correlate this information with the 3D geometrical data. Indeed, these 3D models can be navigated and manipulated to plan suitable conservation treatment interventions, including during the intervention itself.

In particular, the VIS models enabled the full documentation of the aspect and morphology of the object, including discontinuities on the painted surfaces, cracks, and pigment detachments. The 3D models are photorealistic replicas of the artifact, considering that VIS images undergo chromatic and exposure correction exploiting the 24-color X-Rite ColorChecker Classic Mini[®].

Regarding sack No. 1, through UVL imaging, it is possible to discriminate the presence of two main materials on the surface through their fluorescence color. Indeed, on the front side, it is possible to observe a bright light-blueish fluorescence that could be consistent with the presence of synthetic materials, such as acrylic or vinyl resins, applied in previous interventions as a consolidant [37,38]. Indeed this response is detected along the border of the detached painted surface, where the wood is exposed. A representative area is indicated by a white arrow in Figure 5b. In addition, the remaining painted surface presents a blueish response, also detected in correspondence with the area from which a micro-sample was collected. A representative area is indicated by a green arrow in Figure 5b. This result is in accordance with the FTIR analysis, suggesting the possible presence of cellulose nitrate and other organic substance, probably of synthetic origin. In addition, oxalates were also detected, neither excluding nor confirming the presence of other natural organic substances now degraded. Additionally, on the back of the artifact (Figure 5f, black arrow), a wide area presented a yellow fluorescence response in coincidence with the exposed preparation

layer, realized as a mixture of calcium carbonate, as confirmed by the XRF analysis and organic binders, such as vegetable gums or animal glues [36]. In the UVR model, the areas covered in whitish deposits presented a light-grey reflective response (Figure 5c,g). These areas can be discriminated more clearly in the UVR-FC model, in which the information from VIS and UVR images are combined and where a light-blue color characterizes them (Figure 5d,h). A representative area is indicated by a red arrow in Figure 5a,c,d).

Analogous to sack No. 1, on the UVL 3D model of sack No. 2 it is possible to observe areas with a bright light-blueish response to ultraviolet radiation that could be related to a synthetic material, i.e., a consolidant [37,38]. These areas are located on the front and top of the artifact, along the detachment of the painted layer, where the wood is exposed (Figure 6b), and in isolated areas on the back of the item (Figure 6f). A representative area is indicated by a white arrow in Figure 6b. Besides these areas, the overall surface responds to ultraviolet radiation in a non-homogeneous form, with differences in luminescence behavior. In particular, in the front part, some areas have a dark response, suggesting that these areas absorb UV radiation (Figure 6b, blue arrow). Furthermore, on the front side, the overall surface has a blueish response, which could indicate the presence of an organic substance, probably of synthetic origin, in accordance with the FTIR results, analogous to the results of sack No. 1 (Figure 6f, green arrow). Eventually, certain areas have a yellowish response, possibly related to the absence of coating or varnishes. An example can be observed in the upper left part on the back part of the artifact (Figure 6f, yellow arrow). Also, for this artifact, the UVR model can detect the distribution on the surface of materials applied in the outermost layers. In particular, it is possible to find a spatial correlation between the presence of the whitish deposits on the surface detected in the VIS model and a light-grey reflective response in the UVR model (Figure 6c,g). The two pieces of information are combined and easier to read in the UVR-FC model, where these areas appear light-blue in color (Figure 6e,g,h, red arrow). In addition, this latter model emphasizes the distribution of materials with a different surface trend compared to polychromy, allowing the observation of some brushstrokes (Figure 6d,h).

4. Conclusions

This paper presents an innovative analytical user-friendly approach for generating multispectral 3D models. In particular, the aim is to integrate and combine data collected by photogrammetry and multispectral imaging. These techniques are applied with a specific portable and affordable set-up that allows keeping the camera and artifact in a relatively fixed orientation to obtain a multispectral 3D model that can be navigated in a single coordinate system. In addition, the approach involves using Meshroom, an open-source software that allows the creation of textured 3D models.

The approach was applied to the study and investigation of two wooden artifacts from the Museo Egizio di Torino. The combined data on the 3D model, together with close observation of the artifacts, revealed that the artifacts do not present a homogeneous finishing layer. On the contrary, the surface is characterized by strong material non-uniform distribution due to the state of preservation of the artifacts and previous interventions. Indeed, the items are covered by deposits and environmental particles due both to natural degradation and/or to previous interventions. The results obtained with the 3D imaging approach were also confirmed by portable, non-invasive X-ray fluorescence and Fourier-transform infrared spectroscopy.

The information gathered with this approach proved that an integrated 3D model can be employed as an active diagnostic tool by scientists and conservators, not only to archive and preserve the item's aspects. Indeed, the multispectral 3D model allowed the conservators to evaluate the state of preservation of these artifacts and, therefore, to plan interventions and detect areas that could be investigated with additional techniques or that could require sampling.

Author Contributions: Conceptualization, L.E.S., L.L., P.B., A.L.G., A.R. and S.G.; methodology, L.E.S. and L.L.; validation, L.E.S. and L.L.; investigation, L.E.S. and L.L.; resources, P.B., T.C., A.L.G., A.R., M.B., S.A. and S.G.; data curation, L.E.S. and L.L.; writing—original draft preparation, L.E.S.; writing—review and editing, L.E.S., L.L., P.B., T.C., A.L.G., A.R., M.B., S.A. and S.G.; visualization, L.E.S., L.L., P.B. and S.G.; supervision, P.B. and S.G.; project administration, P.B., M.B., S.A. and S.G. All authors have read and agreed to the published version of the manuscript.

Funding: This research received no external funding.

Institutional Review Board Statement: Not applicable.

Informed Consent Statement: Not applicable.

Data Availability Statement: The data presented in this article are available on request from the corresponding author.

Acknowledgments: The authors would like to acknowledge the scientific laboratories of the Centro Conservazione e Restauro “La Venaria Reale” for their support.

Conflicts of Interest: The authors declare no conflict of interest.

Abbreviations

The following abbreviations are used in this manuscript:

MSI	Multispectral Imaging
CH	Cultural Heritage
PG	Photogrammetry
VIS	Visible-reflected
UV	Ultraviolet
UVL	Ultraviolet-induced Visible Luminescence
UVR	Ultraviolet-reflected
UVR-FC	UVR False Color
FTIR	Fourier-transform infrared spectroscopy
XRF	X-ray fluorescence spectroscopy
VIL	Visible-induced Infrared Luminescence
DSLR	digital single-lens reflex

References

1. Artioli, G. *Scientific Methods and Cultural Heritage: An Introduction to the Application of Materials Science to Archaeometry and Conservation Science*; OUP: Oxford, UK, 2010.
2. Es Sebar, L.; Iannucci, L.; Gori, C.; Re, A.; Parvis, M.; Angelini, E.; Grassini, S. In-situ multi-analytical study of ongoing corrosion processes on bronze artworks exposed outdoor. *Acta IMEKO* **2021**, *10*, 241–249. [[CrossRef](#)]
3. Remondino, F.; El-Hakim, S. Image-based 3D Modelling: A Review. *Photogramm. Rec.* **2006**, *21*, 269–291. [[CrossRef](#)]
4. Karastoyanov, D.; Stoimenov, N.; Gyoshev, S. Innovative Approach for 3D Presentation of Plane Culturally-Historical Objects by Tactile Plates for Disadvantaged Users (low-sighted or visually impaired). *Proc. MATEC Web Conf. EDP Sci.* **2019**, *292*, 03004. [[CrossRef](#)]
5. Santos, P.; Ritz, M.; Fuhrmann, C.; Fellner, D. 3D mass digitization: A milestone for archeological documentation. *Virtual Archaeol. Rev.* **2017**, *8*, 1–11. [[CrossRef](#)]
6. Mugnai, F.; Tucci, G.; Da Re, A. Digital image correlation in assessing structured-light 3D scanner’s gantry stability: Performing david’s (michelangelo) high-accuracy 3D survey. *The International Archives of Photogrammetry. Remote Sens. Spat. Inf. Sci.* **2021**, *46*, 463–469. [[CrossRef](#)]
7. Yilmaz, H.M.; Yakar, M.; Gulec, S.A.; Dulgerler, O.N. Importance of digital close-range photogrammetry in documentation of cultural heritage. *J. Cult. Herit.* **2007**, *8*, 428–433. [[CrossRef](#)]
8. Dyer, J.; Verri, G.; Cupitt, J. *Multispectral Imaging in Reflectance and Photo-Induced Luminescence Modes: A User Manual*; British Museum: London, UK, 2013.
9. Hassan, A.T.; Fritsch, D. Integration of Laser Scanning and Photogrammetry in 3D/4D Cultural Heritage Preservation—A Review. *Int. J. Appl.* **2019**, *9*, 76–91.
10. Russo, M.; Remondino, F.; Guidi, G. Principali tecniche e strumenti per il rilievo tridimensionale in ambito archeologico. *Archeol. Calc.* **2011**, *22*, 169–198.

11. Bianco, G.; Gallo, A.; Bruno, F.; Muzzupappa, M. A comparison between active and passive techniques for underwater 3D applications. *Int. Arch. Photogramm. Remote Sens. Spat. Inf. Sci.* **2011**, *34*, 357–363. [[CrossRef](#)]
12. Gonzalez-Jorge, H.; Riveiro, B.; Armesto, J.; Arias, P. Verification artifact for photogrammetric measurement systems. *Opt. Eng.* **2011**, *50*, 073603. [[CrossRef](#)]
13. Beraldin, J.A.; Blais, F.; El-Hakim, S.; Cournoyer, L.; Picard, M. Traceable 3D imaging metrology: Evaluation of 3D digitizing techniques in a dedicated metrology laboratory. In Proceedings of the 8th Conference on Optical 3-D Measurement Techniques, Zurich, Switzerland, 9–12 July 2007.
14. Mathys, A.; Jadinon, R.; Hallot, P. Exploiting 3D multispectral texture for a better feature identification for cultural heritage. *ISPRS Annals of the Photogrammetry. Remote Sens. Spat. Inf. Sci.* **2019**, *4*, 91–97. [[CrossRef](#)]
15. Moropoulou, A.; Zendri, E.; Ortiz, P.; Delegou, E.T.; Ntoutsis, I.; Balliana, E.; Becerra, J.; Ortiz, R. Scanning microscopy techniques as an assessment tool of materials and interventions for the protection of built cultural heritage. *Scanning* **2019**, *2019*, 5376214. [[CrossRef](#)] [[PubMed](#)]
16. Iannucci, L.; Lombardo, L.; Parvis, M.; Cristiani, P.; Basséguy, R.; Angelini, E.; Grassini, S. An imaging system for microbial corrosion analysis. In Proceedings of the 2019 IEEE International Instrumentation and Measurement Technology Conference (I2MTC 2019), Auckland, New Zealand, 20–23 May 2019; pp. 1–6.
17. Iannucci, L.; Parvis, M.; Cristiani, P.; Ferrero, R.; Angelini, E.; Grassini, S. A Novel Approach for Microbial Corrosion Assessment. *IEEE Trans. Instrum. Meas.* **2019**, *68*, 1424–1431. [[CrossRef](#)]
18. Cavaleri, T.; Buscaglia, P.; Caliri, C.; Ferraris, E.; Nervo, M.; Romano, F.P. Below the surface of the coffin lid of Neskhonsuennekhy in the Museo Egizio collection. *X-Ray Spectrom.* **2021**, *50*, 279–292. [[CrossRef](#)]
19. Nicolas, T.; Gagne, R.; Tavernier, C.; Petit, Q.; Gouranton, V.; Arnaldi, B. Touching and interacting with inaccessible cultural heritage. *Presence* **2015**, *24*, 265–277. [[CrossRef](#)]
20. Ju, Y.; Qi, L.; He, J.; Dong, X.; Gao, F.; Dong, J. MPS-Net: Learning to recover surface normal for multispectral photometric stereo. *Neurocomputing* **2020**, *375*, 62–70. [[CrossRef](#)]
21. Lv, J.; Guo, H.; Chen, G.; Liang, J.; Shi, B. NeuralMPS: Non-Lambertian Multispectral Photometric Stereo via Spectral Reflectance Decomposition. *arXiv* **2022**, arXiv:2211.15311.
22. Triolo, P.A.M. *Manuale Pratico di Documentazione e Diagnostica per Immagine per i BB. CC*; Il Prato: Padova, Italy, 2019.
23. Webb, E.K. Optimising Spectral and 3D Imaging for Cultural Heritage Documentation Using Consumer Imaging Systems. Ph.D. Thesis, University of Brighton, Brighton, UK, 2020.
24. Cosentino, A. Identification of pigments by multispectral imaging; a flowchart method. *Herit. Sci.* **2014**, *2*, 8. [[CrossRef](#)]
25. Pelagotti, A.; Pezzati, L.; Piva, A.; Del Mastio, A. Multispectral UV fluorescence analysis of painted surfaces. In Proceedings of the 2006 14th European Signal Processing Conference, Florence, Italy, 4–8 September 2006; pp. 1–5.
26. Nocerino, E.; Rieke-Zapp, D.H.; Trinkl, E.; Rosenbauer, R.; Farella, E.; Morabito, D.; Remondino, F. Mapping VIS and UVL imagery on 3D geometry for non-invasive, non-contact analysis of a vase. *Int. Arch. Photogramm. Remote Sens. Spat. Inf. Sci.* **2018**, *42*, 773–780. [[CrossRef](#)]
27. Fuster-López, L.; Stols-Witlox, M.; Picollo, M. *UV-Vis Luminescence Imaging Techniques. Técnicas de Imagen de Luminiscencia UV-Vis*; Editorial Universitat Politècnica de València: Valencia, Spain, 2020.
28. Jones, C.; Duffy, C.; Gibson, A.; Terras, M. Understanding multispectral imaging of cultural heritage: Determining best practice in MSI analysis of historical artefacts. *J. Cult. Herit.* **2020**, *45*, 339–350. [[CrossRef](#)]
29. Liang, H. Advances in multispectral and hyperspectral imaging for archaeology and art conservation. *Appl. Phys. A* **2012**, *106*, 309–323. [[CrossRef](#)]
30. Hedeard, S.B.; Brøns, C.; Drug, I.; Saulins, P.; Bercu, C.; Jakovlev, A.; Kjær, L. Multispectral Photogrammetry: 3D models highlighting traces of paint on ancient sculptures. In Proceedings of the DHN, Copenhagen, Denmark, 5–8 March 2019; pp. 181–189.
31. Radpour, R.; Fischer, C.; Kakoulli, I. A 3D modeling workflow to map ultraviolet- and visible-induced luminescent materials on ancient polychrome artifacts. *Digit. Appl. Archaeol. Cult. Herit.* **2021**, *23*, e00205. [[CrossRef](#)]
32. Lanteri, L.; Agresti, G.; Pelosi, C. A new practical approach for 3D documentation in ultraviolet fluorescence and infrared reflectography of polychromatic sculptures as fundamental step in restoration. *Heritage* **2019**, *2*, 207–215. [[CrossRef](#)]
33. Triolo, P.A.; Spingardi, M.; Costa, G.A.; Locardi, F. Practical application of visible-induced luminescence and use of parasitic IR reflectance as relative spatial reference in Egyptian artifacts. *Archaeol. Anthropol. Sci.* **2019**, *11*, 5001–5008. [[CrossRef](#)]
34. Zitman, M.J.W.H. The Necropolis of Assiut: A Case Study of Local Egyptian Funerary Culture from the Old Kingdom to the End of the Middle Kingdom. Ph.D. Thesis, Leiden University, Leiden, The Netherlands, 2006.
35. AliceVision. Meshroom—3D Reconstruction Software. Available online: <https://alicevision.org/#meshroom>. Last checked on November (accessed on 2 December 2021).
36. Nicholson, P.T.; Shaw, I. *Ancient Egyptian Materials and Technology*; Cambridge University Press: Cambridge, UK, 2000.

37. Longoni, M.; Buttarelli, A.; Gargano, M.; Bruni, S. A Multiwavelength Approach for the Study of Contemporary Painting Materials by Means of Fluorescence Imaging Techniques: An Integration to Spectroscopic Methods. *Appl. Sci.* **2022**, *12*, 94. [[CrossRef](#)]
38. Ludwig, N.; Orsilli, J.; Bonizzoni, L.; Gargano, M. UV-IR image enhancement for mapping restorations applied on an Egyptian coffin of the XXI Dynasty. *Archaeol. Anthropol. Sci.* **2019**, *11*, 6841–6850. [[CrossRef](#)]

Disclaimer/Publisher’s Note: The statements, opinions and data contained in all publications are solely those of the individual author(s) and contributor(s) and not of MDPI and/or the editor(s). MDPI and/or the editor(s) disclaim responsibility for any injury to people or property resulting from any ideas, methods, instructions or products referred to in the content.